(13) J. D. Kennedy and W. McFarlane, *Mol. Phys.*, **29**, 593 (1975).
(14) M. Barfield and D. M. Grant, *J. Chem. Phys.*, **67**, 3322 (1977). In these results, calculated diamagnetic shielding components agreed with ab initio values to generally better than 1%.
(15) S. G. Kukolich, *Phys. Rev. A*, **138**, 1322 (1965).
(16) J. P. Gordon, *Phys. Rev.*, **99**, 1253 (1955).
(17) J. H. Van Vleck, *Rev. Mod. Phys.*, **23**, 213 (1951).
(18) A. R. Edmonds, "Angular Momentum in Quantum Mechanics", Princeton University Press, Princeton, N.J., 1960.
(19) P. Thaddeus, L. C. Krisher, and J. H. N. Loubser, *J. Chem. Phys.*, **40**, 257 (1964).
(20) P. Thaddeus, L. C. Krisher, and P. Cahill, *J. Chem. Phys.*, **41**, 1542 (1964).

(21) S. G. Kukolich, *Phys. Rev.*, **156**, 83 (1967).
(22) W. H. Flygare and J. Goodisman, *J. Chem. Phys.*, **49**, 3122 (1968); T. D. Gierke, H. L. Tigelaar, and W. H. Flygare, *J. Am. Chem. Soc.*, **94**, 330 (1972); T. D. Gierke and W. H. Flygare, *ibid.*, **94**, 7277 (1972).
(23) R. Ditchfield, D. P. Miller, and J. A. Pople, *J. Chem. Phys.*, **54**, 4186 (1971).
(24) A. Pines, M. G. Gibby, and J. S. Waugh, *J. Chem. Phys.*, **59**, 569 (1973); *Chem. Phys. Lett.*, **15**, 373 (1972).
(25) W. T. Raynes, A. D. Buckingham, and H. J. Bernstein, *J. Chem. Phys.*, **36**, 3481 (1962).
(26) K. Jackowski and W. T. Raynes, *Mol. Phys.*, **34**, 465 (1977); B. Tiffon and J. P. Doucet, *Can. J. Chem.*, **54**, 2045 (1976); D. Cans, B. Tiffon, and J. E. Dubois, *Tetrahedron Lett.*, 2075 (1976).

Calculated ¹³C NMR Relaxation Parameters for a Restricted Internal Diffusion Model. Application to Methionine Relaxation in Dihydrofolate Reductase

Robert E. London* and John Avitabile

Contribution from Los Alamos Scientific Laboratory, University of California, Los Alamos, New Mexico 87545. Received April 19, 1978

Abstract: ¹³C NMR relaxation parameters, T_1, T_2, and NOE, have been calculated based on a model assuming internal rotational diffusion subject to boundary conditions limiting the range of motion. Numerical results are presented as a function of diffusion coefficients D_0 and D_i and the angle β defined as in the free internal rotation calculation, as well as 2θ, the allowed range of motion. Relaxation times vary from the values expected in the absence of internal motion to values slightly below those calculated using the free internal rotation model as the range is increased from 0 to 360°. The discrepancy in the latter comparison arises from the boundary condition preventing diffusion from 180⁺ to 180⁻. Changes in T_2 are typically monotonic or nearly monotonic as a function of θ; however, changes in T_1 and NOE values are markedly nonmonotonic for $D_0 \lesssim 10^6 \, \text{s}^{-1}$ and for certain values of D_i. Criteria for the applicability of the present calculations to the analysis of ¹³C NMR relaxation data obtained in studies of macromolecules undergoing restricted internal motion have been suggested. The results have been generalized to the case of multiple internal rotations, specifically for the problem of one free and one restricted diffusional process. In general, the two types of rotation are not commutative. This model has been applied to relaxation data recently obtained for the methionine methyl resonances of specifically ¹³C-labeled dihydrofolate reductase obtained from *S. faecium*. The results indicate that the data can be readily explained by assuming rapid free internal diffusion about the S–CH₃ bond and restricted internal diffusion about the CH₂–S bond of methionine, such that for the broadest resonances the motional range is restricted to ~90° and for the sharpest resonances the range is >180°. Restriction of the motion allows a significantly better fit of the data than can be obtained using a model based on two free internal rotations.

I. Introduction

The use of NMR relaxation measurements to obtain dynamic information is based on models which relate the calculated spectral densities to the relevant physical parameters. Models currently in use can be divided into two categories: (1) diffusion over a continuum (isotropic or anisotropic) as described by a diffusion equation[1-9] or by collision theory[10] and (2) jumps between several discrete states. The second class has been developed extensively to describe the relaxation effects of jumps between discrete states in a variety of solids[11] and group-theoretical methods have recently been applied to obtain general solutions.[12] Applications to macromolecules for which overall diffusion is also important have also been developed.[1,13-17] We have recently shown that a two-state jump model superimposed on overall isotropic diffusion provides a satisfactory approach for the calculation of spin lattice relaxation rates due to ring puckering in proline-containing peptides.[18] Both approaches have been generalized to a series of successive rotations[14,19] or jumps[14,17,20] applicable to complex biomolecules. In the present study, a third type of model is considered: free internal diffusion over a restricted range imposed by boundary conditions on the solution of the diffusion equation. Computationally, this approach differs from previous work[21] in that the relevant autocorrelation

function must be expressed as an infinite series of exponentials. Fortunately, the series is rapidly convergent so that typically only a few terms need be considered. It is thus relatively easy to obtain numerical results for the desired relaxation parameters.

The need for an understanding of the contribution of restricted diffusion to nuclear magnetic relaxation rates arises primarily in the study of complex biomolecules in which restricted internal motion of parts of the molecule is the rule rather than the exception. For example, recent ¹³C NMR studies of 90% methionine-*methyl*-¹³C labeled dihydrofolate reductase from *S. faecium*[22] indicate that internal motion in addition to the expected rapid methyl rotation is significant. Alternatively, the data cannot be explained by using a model which assumes free (unrestricted) rotation about two or more bonds. It was also found that sharper peaks exhibit longer ¹³C T_1 values and somewhat larger NOE values than broader peaks. However, models based on one or more free internal rotations predict that if the overall motion is in the slow tumbling region, faster internal motion leads to longer T_1 values but smaller NOE values.[7,23] Thus, explanations of these results using models in which only the rates of internal or overall motion can be varied cannot accommodate the data. The present calculation, while employing idealized boundary conditions, provides a reasonable interpretation of this data
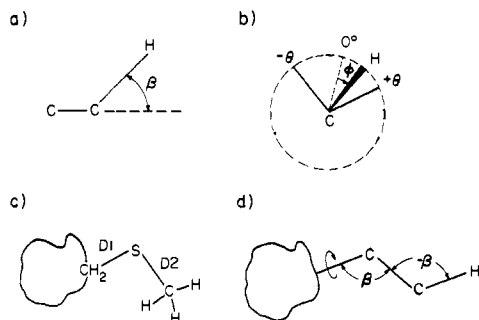
Figure 1. (a) Illustration of the angle β defined by the internal rotation axis assumed to be coincident with a carbon–carbon bond and by the C–H relaxation vector. Note: Since $|d_{i,j}(\beta)|^2 = |d_{i,-j}(180° - \beta)|^2$, spectral densities of the form of eq 16 and 25 are valid for β or $180° - \beta$. (b) View parallel to the C–C bond of (a) illustrating the azimuthal angle ϕ and the boundaries at $\phi = \pm\theta$. (c) Illustration of the model used for calculation of relaxation parameters for the methionine methyl carbons in dihydrofolate reductase. The diffusion indicated by D_1 is assumed to be restricted and the diffusion indicated by D_2 unrestricted so that the spectral density has the form of eq 25. (d) Illustration of the diffusion model described by eq 30 and 31. The restricted motion about the second bond is described by $\theta = 0$ and $\beta' = -\beta$ so that the internal diffusion axis is parallel to the C–H relaxation vector. In this limit, the internal motion does not affect the relaxation times.

in terms of free methyl rotation and restricted motion about the preceding CH₂–S bond.

II. Theory

In this section we consider the problem of restricted internal motion about an axis making an angle β with the relevant C–H relaxation vector (Figure 1a). Overall molecular motion is assumed to be isotropic and a dipolar relaxation mechanism for the ^{13}C nuclei due to interaction with directly bonded protons is assumed to be dominant. There are substantial precedents for the validity of these assumptions.[6,24-26] The relevant autocorrelation function can then be written in the form[3,14]

$$G(t) = \sum_{a=-2}^{2} e^{-6D_0 t} |d_{a0}(\beta)|^2 \langle e^{ia[\phi(0)-\phi(t)]} \rangle \tag{1}$$

In the above expression, d_{a0} are reduced second-rank Wigner rotation matrices,[27] β is defined above, D_0 is the isotropic diffusion coefficient, and ϕ represents an azimuthal displacement of the C–H vector about the effective rotation axis. Since we wish to consider a more general problem involving both free and restricted rotations in a subsequent section, we define a matrix $A_{m,m'}$ by analogy with the unrestricted rotation problem to be

$$A_{m,m'} = \langle e^{im\phi(0)\phi} e^{-im'\phi(t)} \rangle \tag{2}$$

Thus, the ensemble average appearing in eq 1 is given by $A_{a,a}$. This ensemble average can be written in the form

$$A_{m,m'}$$
$$= \int_{-\pi}^{\pi} \int_{-\pi}^{\pi} e^{im\phi_0} e^{-im'\phi_t} p(\phi_0) p(\phi_t, t/\phi_0, 0) \, d\phi_0 \, d\phi_t \tag{3}$$

where the abbreviations $\phi_0 = \phi(0)$ and $\phi_t = \phi(t)$ have been used, $p(\phi_0)$ is the probability that ϕ initially has the value of ϕ_0, and $p(\phi_t, t/\phi_0, 0)$ is the conditional probability that if ϕ was initially equal to ϕ_0, it will be equal to ϕ_t at time t. The calculational problem thus is reduced to obtaining the required conditional probability.

The model used for this calculation is based on the angular

diffusion equation

$$\frac{\partial \psi(\phi, t)}{\partial t} = \frac{D}{a^2 \sin^2 \beta} \frac{\partial^2 \psi(\phi, t)}{\partial \phi^2} \tag{4}$$

subject to the boundary conditions

$$\partial\psi/\partial\phi|_{\phi=\theta} = \partial\psi/\partial\phi|_{\phi=-\theta} = 0 \tag{5}$$

and to the initial condition

$$\psi(\phi, t = 0) = \delta(\phi - \phi_0) \tag{6}$$

The boundary condition, eq 5, prevents diffusion across the boundary (Figure 1b). As a result of the initial condition, $\psi(\phi, t)$ becomes the desired conditional probability, $\psi(\phi_t, t/\phi_0, 0)$. In eq 4 D (cm²/s) is the diffusion coefficient and a is the length of the C–H vector for the model illustrated in Figure 1. Equation 4 has the general solution

$$\psi(\phi, t)$$
$$= \left[C_1 \cos \left(\frac{\phi}{(\tau D_i)^{1/2}} \right) + C_2 \sin \left(\frac{\phi}{(\tau D_i)^{1/2}} \right) \right] e^{-t/\tau} + C_3 \tag{7}$$

where C_1, C_2, and C_3 are constants and

$$D_i = D/(a^2 \sin^2 \beta) \tag{8}$$

The above definition of the internal diffusion coefficient is identical with that used in the free internal rotation calculation. Application of boundary and initial conditions is facilitated by transforming to the coordinate system $\phi \rightarrow \phi + \theta$. Transforming back to the original system then gives

$$\psi(\phi_t, t/\phi_0, 0) = \frac{1}{2\theta} + \frac{1}{\theta} \sum_{n=1}^{\infty} \cos \frac{n\pi}{2\theta} (\phi_0 + \theta)$$
$$\times \cos \frac{n\pi}{2\theta} (\phi_t + \theta) \exp(-t/\tau_n) \tag{9}$$

where

$$\tau_n = 4\theta^2/(n^2\pi^2 D_i) \tag{10}$$

We note that in the limit $t \rightarrow \infty$, this result gives $\psi(\phi_t, t/\phi_0, 0) \rightarrow 1/2\theta$ so that given enough time, the probability becomes uniformly distributed over the interval $-\theta < \phi < \theta$. Thus, the a priori probability that $\phi = \phi_0$ at time $t = 0$ is given by

$$p(\phi_0) = 1/2\theta \tag{11}$$

Using the above results in eq 3 then gives (Appendix A)

$$A_{mm'} = \frac{\sin m\theta}{m\theta} \frac{\sin m'\theta}{m'\theta}$$
$$+ \frac{1}{2} \sum_{n=1}^{\infty} \left[\frac{\sin \left(m\theta - \frac{n\pi}{2} \right)}{m\theta - \frac{n\pi}{2}} + (-1)^n \frac{\sin \left(m\theta + \frac{n\pi}{2} \right)}{m\theta + \frac{n\pi}{2}} \right]$$
$$\times \left[\frac{\sin \left(m'\theta - \frac{n\pi}{2} \right)}{m'\theta - \frac{n\pi}{2}} + (-1)^n \frac{\sin \left(m'\theta + \frac{n\pi}{2} \right)}{m'\theta + \frac{n\pi}{2}} \right]$$
$$\exp(-t/\tau_n) \tag{12}$$

The above expression can be written in the form

$$A_{m,m'} = \sum_{n=0}^{\infty} E(m, n) E(m', n) \exp(-t/\tau_n) \tag{13}$$

where $E(m,n)$ is defined by

$$E(m,0) = \frac{\sin m\theta}{m\theta}$$

$E(m,n \neq 0)$

$$= \frac{1}{2^{1/2}} \left[\frac{\sin\left(m\theta - \frac{n\pi}{2}\right)}{m\theta - \frac{n\pi}{2}} + (-1)^n \frac{\sin\left(m\theta + \frac{n\pi}{2}\right)}{m\theta + \frac{n\pi}{2}} \right] \quad (14)$$

This expression gives the required $A_{m,m'}$ matrix for the restricted motion calculation. It may be compared with the analogous expression for the unrestricted internal diffusion calculation:

$$A_{m,m'}{}^{\text{FIR}} = \delta_{m,m'} \exp(-m^2 D_i t) \quad (15)$$

where FIR stands for free internal rotation and D_i is given by eq 8. Although the restricted motion problem leads to an infinite series for the autocorrelation function, the terms in eq 12 drop off as $1/n^2$ leading to rapid convergence of the sum so that in practice numerical results are readily obtained. We also note the result for $\theta \to 0$: $E(m,0) \to 1$, and for $n \neq 0$ $\tau_n \to 0$ so that these terms can be dropped. Thus, in this limit, we can write $E(m,n) \to \delta_{n,0}$.

The spectral densities used to calculate the required relaxation times are obtained by substitution of eq 13 into eq 1 and Fourier transforming the result:

$$J(\omega) = \sum_{a=-2}^{2} \sum_{n=0}^{\infty} |d_{a0}(\beta)|^2 |E(a, n)|^2 \tau/(1 + \omega^2\tau^2) \quad (16)$$

$$\tau = (6D_0 + n^2\pi^2 D_i/4\theta^2)^{-1} \quad (17)$$

Numerical Results. Behavior under Limiting Conditions

Using the spectral density equations 16 and 17 obtained in the previous section, numerical results were obtained corresponding to values of D_0 between 10^6 and 10^{10} s^{-1} ($\tau_0 = 1.67 \times 10^{-7}$ to 1.67×10^{-11} s), D_i in the range 10^9–10^{11} s^{-1}, and several typically encountered values of β. The carbon resonance frequency was set to 25.2 MHz. T_1, T_2, and NOE values were obtained using eq 18–20:

$$\frac{1}{T_1} = \frac{N\gamma_C^2\gamma_H^2\hbar^2}{10r_{CH}^6} [J(\omega_C - \omega_H) + 3J(\omega_C)$$
$$+ 6J(\omega_H + \omega_C)] \quad (18)$$

$$\frac{1}{T_2} = \frac{N\gamma_C^2\gamma_H^2\hbar^2}{20r_{CH}^6} [J(\omega_H - \omega_C) + 3J(\omega_C) + 6J(\omega_H + \omega_C)$$
$$+ 4J(0) + 6J(\omega_H)] \quad (19)$$

$$\text{NOE} = 1 + \eta$$

$$= 1 + \frac{\gamma_H}{\gamma_C} \left[\frac{6J(\omega_H + \omega_C) - J(\omega_H - \omega_C)}{J(\omega_H - \omega_C) + 3J(\omega_C) + 6J(\omega_H + \omega_C)} \right] \quad (20)$$

In the above equations, N is the number of directly bonded protons. Cross correlation effects have not been considered in the present calculation. In general, such effects lead to nonexponential spin lattice relaxation; however, the appropriately weighted initial relaxation rate is that calculated neglecting these effects.[23,28]

Before considering the detailed dependence of the relaxation times on the various motional parameters, we note several qualitative features of the model. First, in the limit $\theta \to 0$, calculated spectral densities and consequently T_1, T_2, and NOE values all approach the values obtained in the absence of internal motion. In particular, using the result $E(a,0) \to 1$ as well as the observation that $n^2\pi^2 D_i/4\theta^2 \to \infty$ so that only

the first term in eq 16 contributes to the sum, we have

$$J(\omega) \xrightarrow[\theta \to 0]{} \sum_{a=-2}^{2} \sum_{n=0}^{\infty} |d_{a0}(\beta)|^2 |E(a,n)|^2 \frac{\tau}{1 + \omega^2\tau^2}$$

$$= \sum_{a=-2}^{2} |d_{a0}(\beta)|^2 \frac{\tau}{1 + \omega^2\tau^2} = \frac{\tau}{1 + \omega^2\tau^2} \quad (21)$$

where the sum rule for the reduced Wigner rotation matrices has been used.[27]

In contrast to the above result, $J(\omega)$ does not approach the value of free internal rotation in the limit $2\theta = 360°$. This reflects the fact that although any value of θ is now permitted, the boundary conditions become a spike at $\theta = 180°$ preventing diffusion from 180^+ to 180^-. However, in the limit $D_1 \to \infty$, so that only the $n = 0$ term in the sum in eq 16 is significant, the limit $2\theta = 360°$ leads to the result

$$J(\omega) \to \left(\frac{3\cos^2\beta - 1}{2} \right)^2 \frac{\tau}{1 + \omega^2\tau^2}; \quad \tau \to (6D_0)^{-1} \quad (22)$$

which is identical with the free internal rotation result in the limit $D_i \to \infty$.

More generally, in the limit $D_i \to \infty$ but imposing no restrictions on ϕ, the $n = 0$ term in eq 16 is dominant leading to the result

$$J(\omega)_{D_i \to \infty} \to \left[\left(\frac{3\cos^2\beta - 1}{2} \right)^2 + 3\sin^2\beta\cos^2\beta\left(\frac{\sin\theta}{\theta}\right)^2 \right.$$
$$\left. + \frac{3}{4}\sin^4\beta\left(\frac{\sin 2\theta}{2\theta}\right)^2 \right] \times \frac{\tau}{1 + \omega^2\tau^2}; \quad \tau = 1/(6D_0) \quad (23)$$

The above expression includes a $(\sin\theta/\theta)^2$ term which decreases monotonically in the region $0 < \theta < 180°$ as well as a $(\sin 2\theta/2\theta)^2$ term which leads to nonmonotonic behavior in this region. The latter term arises from the $\exp(2i\phi)$ term in the Hamiltonian. The relative importance of the $(\sin\theta)/\theta$ and $(\sin 2\theta)/2\theta$ terms is dependent on β. Thus, the ratio of the third term to the second in eq 23 increases as $\sin^2\beta/\cos^2\beta$ increases and is, therefore, maximal for $\beta = 90°$. Nonmonotonic changes in the relaxation parameters as a function of θ are therefore most pronounced for $\beta = 90°$. The particular form obtained for the spectral density is a function of the boundary conditions applied in the solution of the diffusion equation. Differences in the boundary conditions applicable to real physical systems might lead to monotonic behavior. Nevertheless, the present calculation provides perhaps the simplest model for obtaining at least a qualitative understanding of the effects of motional restriction on NMR relaxation parameters.

Illustrative Calculations. Numerical results obtained for NT_2 (N is the number of directly bonded protons with a bond length $r_{CH} = 1.09$ Å assumed) as a function of θ and corresponding to the values of D_0, D_i, and β indicated are summarized in Figure 2. Values of parameters are calculated out to $\theta = 180°$ corresponding to a full range of motion ($2\theta = 360°$). In addition, values obtained using the free internal rotation model and the same motional parameters, D_0, D_i, and β, are indicated. In all cases, agreement between these results and the restricted motion calculation for $\theta = 180°$ is good, although exact agreement is only predicted in the limit $D_i \to \infty$ as noted above. Perhaps the most striking observation is the inflection of several of the curves and the fact that for $\beta = 90°$ the changes are nonmonotonic. This result is consistent with the expected periodicity noted in the previous section.

Numerical results for NT_1 analogous to those for NT_2 are summarized in Figure 3. For motion in the extreme narrowing region, the dependence on θ is qualitatively similar to that of NT_2. However, for $D_0 = 10^6$ s^{-1} and $D_i = 10^{10}$ s^{-1}, a more complex pattern is observed: the NT_1 curve passes through a maximum near $\theta = 57°$. It is apparent from this result that the application of the present model to the analysis of restricted
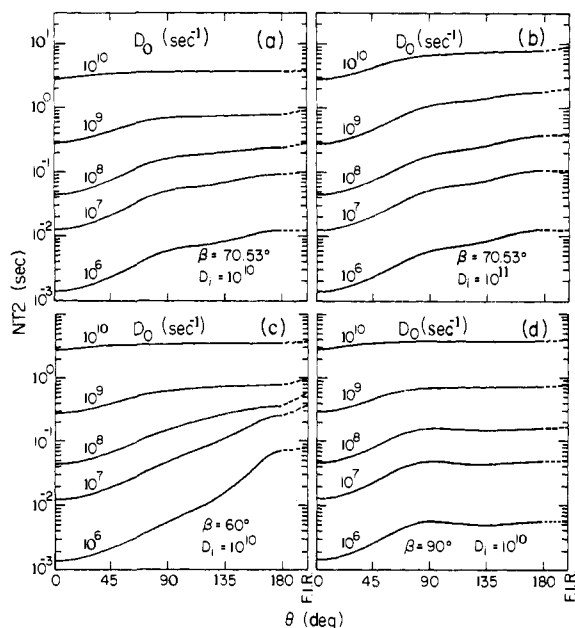
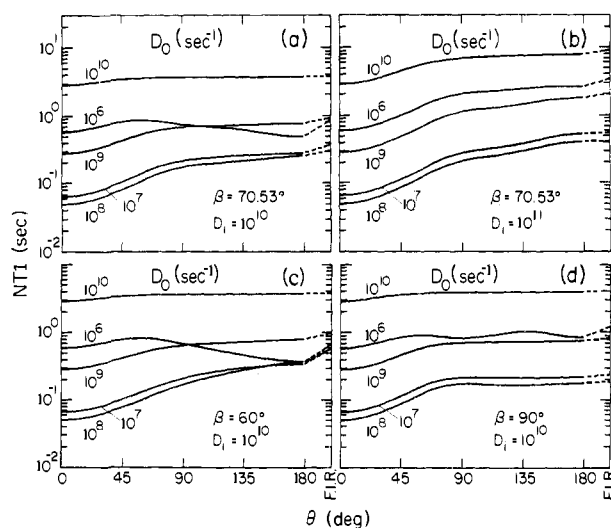Figure 2. NT_2 values plotted as a function of θ for values D_0, D_i, and β indicated. Results are plotted out to $\theta = 180°$ corresponding to a 360° range of motion. Values with the abcissa indicated by FIR correspond to calculations using the free internal rotation model (without boundary conditions) and correspond to the same motional parameters, D_0, D_i, and β. Calculations are for a carbon resonance frequency of 25.2 MHz.

Figure 3. NT_1 values plotted as a function of θ for the D_0, D_i, and β values indicated. FIR values correspond to the free internal rotation model.

internal motion for certain motional parameters is suspect. Clearly, the NT_2 values provide a more useful interpretive tool for motion described by the parameters noted above. We note, however, that for $D_0 = 10^6$ s^{-1} and $D_i = 10^9$ or 10^{11} s^{-1} the curves are again monotonic and correspond to the expected decrease in T_1 in the first case and to the expected increase in the second case. In general, the behavior of the NT_1 curves as a function of θ is most difficult to interpret physically for overall motion D_0 in the slow tumbling range, and is also difficult to interpret if the total expected change in NT_1 on going from no internal motion to free internal motion is small. These conditions apply to the $D_0 = 10^6$ s,$^{-1}$ $D_i = 10^{10}$ s^{-1} case.

NOE calculations exhibit the same difficulties as the NT_1 calculations for overall motion in the slow tumbling range (Figure 4). We first note that even in the free internal rotation case the dependence of the NOE on the various motional parameters is complex. For overall motion in the slow tumbling limit, internal motion characterized by a diffusion coefficient $D_i = 10^9$ s^{-1} leads to the most pronounced increase in NOE; faster or slower internal diffusion produces a smaller increase. For $D_0 = 10^6$ s^{-1} and various values of D_i and β, the deviations from monotonic behavior are most significant. For $D_0 \gtrsim 10^7$ s^{-1}, the deviations are less pronounced and generally the $\theta = 180°$ value is within 10% of the free internal rotation value. Since experimental determinations are generally accurate to only ~10%, this limitation does not seem severe.

On the basis of the illustrative calculations presented above, it is apparent that application of the present model to the analysis of relaxation data obtained for typical macromolecules in terms of restricted motion is not straightforward in all cases. This is particularly true if the relaxation parameters are nonmonotonic functions of θ. In most, although not all, cases examined, we note that markedly nonmonotonic behavior in the NT_1 and NOE calculations is correlated with poor agreement between the values corresponding to a full range of internal motion ($2\theta = 360°$) and the free internal rotation calculation.

As noted in the previous section, the detailed behavior of the calculated relaxation parameters is dependent on the boundary

conditions assumed. For calculations in which the parameters for $\theta = 180°$ are in poor agreement with the free internal rotation values, the existence of an infinite barrier at $\theta = 180°$ apparently has a significant effect on the calculations. Thus, application of the model corresponding to these parameters will produce results of uncertain validity. Furthermore, in view of the correlation between nonmonotonic behavior and poor agreement in the free rotation limit noted above, the present model may be double- or triple-valued in the region of interest. We, therefore, conclude that application of the present calculational model to problems of practical interest is valid only for diffusion coefficients for which the agreement of the $\theta = 180°$ calculation and the free internal rotation calculation is reasonably close and for which changes in NT_1 and NOE with θ are nearly monotonic. Fortunately, these criteria appear to be satisfied for a number of typically encountered cases, including small proteins (mol wt 20 000) with rotational correlation times of ~20 ns.

Perhaps the most significant features of the calculated relaxation parameters are the small changes observed for $\theta < 25°$. Thus, substantial freedom of internal motion corresponding to a range of nearly 50° produces relatively little effect on the calculated T_1, T_2, or NOE values. This result suggests that for a particle in a harmonic well which spends proportionately more time near $\phi = 0$, such restricted diffusional motion will have even less of an effect. Most of the changes in the relaxation parameters occurs in the region 45° $< \theta < 90°$. These results suggest in general that occasional large angular displacements dominate the relaxation effects monitored by NMR. This conclusion is reasonable in light of ^{13}C NMR data. Thus, T_1 values for the α carbons of various proteins typically correspond to isotropic rotational correlation times expected for the entire macromolecule[26,29-32] although these carbons undoubtedly undergo significant but relatively restricted internal motion.[33]

Multiple Internal Rotations. Application to the Relaxation of Methionine Residues in Dihydrofolate Reductase. In a recent study of 90% methionine-*methyl*-^{13}C labeled dihydrofolate reductase it was noted that the methyl relaxation parameters obtained suggest free rotation of the methyl groups as well as additional but restricted motion about another molecular bond, most likely the CH_2–S bond of methionine.[22] The theory of multiple internal rotations developed by Wallach[14] can be readily extended to the case in which one of the motions is restricted. Assuming that the two motions are uncorrelated— which we believe to be a valid assumption for the present
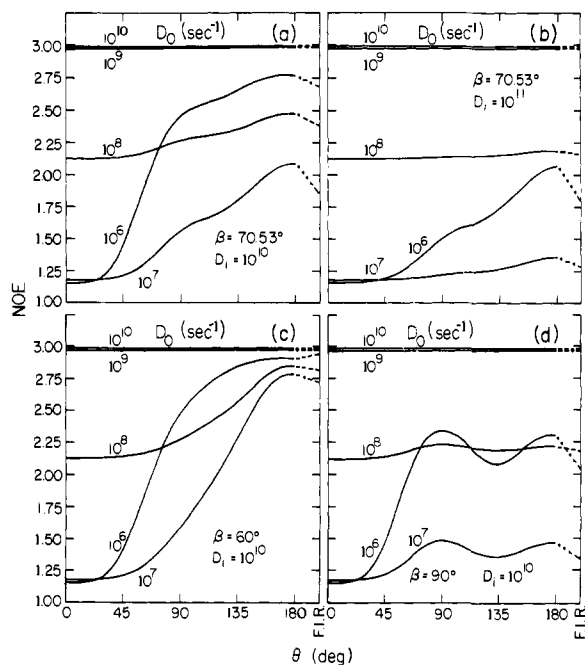
Figure 4. ^{13}C-{^{1}H} nuclear Overhauser enhancement (NOE) values plotted as a function of θ for the D_0, D_i, and β values indicated. FIR values correspond to the free internal rotation model.

problem—the orientational autocorrelation function has the form

$$G(t) = \sum_{a,b,b',c,c'} \mathbf{d}_{ab}(\beta_0)\mathbf{d}_{ab'}(\beta_0)\mathbf{A}^1{}_{bb'}\mathbf{d}_{bc}(\beta)$$

$$\times \mathbf{d}_{b'c'}(\beta)\mathbf{A}^2{}_{cc'}\mathbf{d}_{c0}(\beta')\mathbf{d}_{c'0}(\beta')\,e^{-6D_0 t} \quad (24)$$

where the $\mathbf{d}_{ab}(\beta)$ are the reduced Wigner rotation matrices used above and the remaining parameters are defined as in the free rotation case. The first summation index a is repeated since the overall motion is assumed to be isotropic. The angles β_0 and β correspond to angles between successive internal rotation axes and the angle β' is defined by the final internal rotation axis and the C–H relaxation vector. β_0 is defined arbitrarily but is eliminated from the calculations due to the sum over a. Although the problem solved by Wallach makes use of eq 15 for the **A** matrix, there is no constraint preventing the use of different models for the two rotations leading to different expressions for $\mathbf{A}^1$ and $\mathbf{A}^2$. It is first necessary to note that if one rotation is assumed free and the second restricted, the results are not commutative. In the calculation for methionine labeled dihydrofolate reductase, we assume $\mathbf{A}^1$ corresponds to restricted motion and $\mathbf{A}^2$ to the free methyl rotation. The latter assumption introduces a $\delta_{c,c'}$, into the calculation. Further, using the sum rule for the Wigner rotation matrices,[27] the sum over a gives $\delta_{b,b'}$. We then have

$$G(t) = \sum_{b,c=-2}^{+2} \sum_{n=0}^{\infty} |E(b,n)|^2|\mathbf{d}_{bc}(\beta)|^2|\mathbf{d}_{c0}(\beta')\beta|^2$$

$$\times \exp\left[-\left(6D_0 + \frac{n^2\pi^2 D_1}{4\theta^2} + c^2 D_2\right)t\right] \quad (25)$$

where D_1 corresponds to the restricted motion diffusion process and D_2 corresponds to the free diffusion process. We note that in the limit $\theta \to 0$; we expect that the results should approach those obtained for an isotropically tumbling molecule with a single free internal rotation. This is borne out using the results that in this limit, $E(b,0) \to 1$, and all other terms in the sum

over n vanish since the term $n^2\pi^2 D_1/(4\theta^2) \to \infty$. Thus,

$$G(t)_{\theta \to 0} \to \sum_{b,c=-2}^{+2} \sum_{n=0}^{\infty} \delta_{n0}|\mathbf{d}_{bc}(\beta)|^2|\mathbf{d}_{c0}(\beta)|^2|^2$$

$$\times \exp\left[-\left(6D_0 + \frac{n^2\pi^2 D_1}{4\theta^2} + c^2 D_2\right)t\right]$$

$$= \sum_{c=-2}^{2} |\mathbf{d}_{c0}(\beta')|^2 \exp[-(6D_0 + c^2 D_2)t] \quad (26)$$

as expected.

In contrast to the above results, if the first motion is free and the second restricted, the autocorrelation function has the form

$$G(t) = \sum_{b,c,c'=-2}^{2} \sum_{n=0}^{\infty} \mathbf{d}_{bc}(\beta)\mathbf{d}_{bc'}(\beta)E(c,n)E(c',n)$$

$$\times \mathbf{d}_{c0}(\beta')\mathbf{d}_{c'0}(\beta') \exp\left[-\left(6D_0 + b^2 D_1 + \frac{n^2\pi^2 D_2}{4\theta^2}\right)t\right] \quad (27)$$

As above, we can consider the effect of restricting θ to 0. Making use of the behavior of $E(c,n)$ in this limit, we obtain

$$G(t)_{\theta \to 0} \to \sum_{b,c,c'} \mathbf{d}_{bc}(\beta)\mathbf{d}_{bc'}(\beta)\mathbf{d}_{c0}(\beta')\mathbf{d}_{c'0}(\beta')$$

$$\times \exp[-(6D_0 + b^2 D_1)t] \quad (28)$$

It is apparent physically that if the second rotation is restricted to zero range, the system should behave as if only one free internal rotation were permitted. In this case, however, the angle between the relaxation C–H vector and the axis of rotation depends on both β and β'. For the case $\beta' = -\beta$ (Figure 1d), the internal motion should produce no effect since the axis of internal rotation is parallel to the C–H vector. Setting $\beta' = -\beta$ and using the relation for the Wigner rotation matrices[27]

$$\mathbf{d}_{m,n}{}^j(\beta) = \mathbf{d}_{n,m}{}^j(-\beta) \quad (29)$$

we obtain

$$G(t) = \sum_{b,c,c'=-2}^{+2} \mathbf{d}_{bc}(\beta)\mathbf{d}_{bc'}(\beta)\mathbf{d}_{0c}(\beta)\mathbf{d}_{0c'}(\beta)$$

$$\times \exp[-(6D_0 + b^2 D_1)t] \quad (30)$$

Using the sum rule noted previously and performing the sums over c and c' then gives:

$$G(t) = \sum_{b} \delta_{b0}\delta_{b0} \exp[-(6D_0 + b^2 D_1)t] = \exp[-(6D_0 t)]$$

$$(31)$$

as expected.

We next consider the application of the present calculation to the relaxation of the methionine methyl carbons in dihydrofolate reductase. On the basis of the crystal structure of methionine,[34] we have taken $\beta = 100°$ and assumed $\beta' = 109.5°$. On the basis of eq 25 and the parameter $D_0 = 8.33 \times 10^6$ s^{-1} ($\tau_0 = 2 \times 10^{-8}$ s) determined from measurements on the arginine labeled enzyme,[35] D_1 and D_2 were varied to fit the data. Relaxation parameters for the narrower methionine methyl peaks can be predicted with reasonable accuracy using a model which assumes two free internal rotations most probably corresponding to motion about the S–CH$_3$ and CH$_2$–S bonds.[22] However, for the broader peaks with lower NOE, the present model leads to a significantly better fit. One series of calculations is summarized in Table I. We note that using the present theory, parameters corresponding to all of the methionine residues can be calculated using a given set of D_1 and D_2 values and varying only the range of motion about the CH$_2$–S bonds. In particular, using the data reported previously,[22] the present calculation gives good agreement using
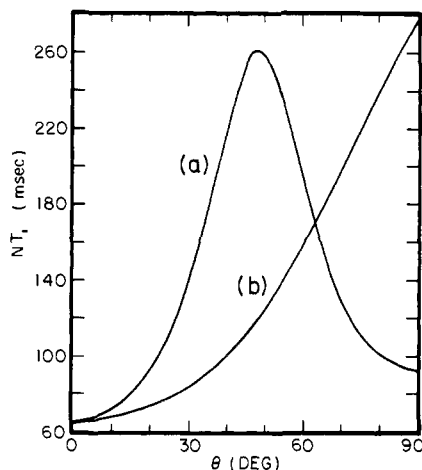
Figure 5. Calculated NT_1 values for (a) a two-state model as described in ref 18 with parameters $D_0 = 10^7$ s^{-1}, $\beta = 70.53°$, and $\tau_A = \tau_B = 1.67 \times \omega^{-12}$ s and (b) a restricted diffusion model as developed here with $D_0 = 10^7$ s^{-1}, $\beta = 70.53°$, and $D_1 = 10^{11}$ s^{-1}; results are plotted as a function of θ.

Table I. Theoretical ^{13}C NMR Parameters for a Model (Equation 25) Corresponding to Methionine Relaxation in Dihydrofolate Reductase

θ, deg	NT_1, s	NT_2, s	NOE
0	0.587	0.094	1.42
25	0.696	0.113	1.44
45	0.973	0.165	1.53
50	1.072	0.186	1.56
55	1.180	0.210	1.60
60	1.294	0.237	1.65
65	1.407	0.266	1.70
70	1.513	0.294	1.75
75	1.603	0.321	1.79
80	1.673	0.342	1.82
85	1.721	0.358	1.85
90	1.748	0.366	1.86
135	1.764	0.362	1.83
180	1.900	0.422	1.94

^{a} Calculations based on $D_0 = 8.33 \times 10^6$ s^{-1}, $D_1 = 2.0 \times 10^{10}$ s^{-1}, $D_2 = 4.0 \times 10^{10}$ s^{-1}, $\beta = 80°$ (complement of 100°), and $\beta' = 70.53°$ (complement of the tetrahedral angle).

$D_1 = 2 \times 10^{10}$ s^{-1}, $D_2 = 4 \times 10^{10}$ s^{-1}, and a range of motion (2θ) varying from ~100° for the broadest peaks to 180–360° for the narrower peaks. For example, for the methionine resonance furthest upfield in the enzyme–methotrexate binary complex measured relaxation parameters $NT_1 = 1.11$ s, $\nu = 5$ Hz ($NT_2 = 191$ ns) and NOE $\approx 1.6^{22}$ are in close agreement with the entry in Table I for $\theta = 55°$. The fit can be improved slightly if D_1 and D_2 are allowed to vary; however, the parameters noted cover the whole range of data reasonably well (Table II of ref 22). These values should not be taken too literally, however, since, as we have noted, the details of the theoretical results obtained here are dependent on the particular boundary conditions assumed. We can conclude, however, that a model of the present type is capable of providing a significantly better description of the relaxation data than a model assuming either one or two free internal rotations. It is also clear that differences in the allowed range of motion rather than differences in the diffusion rates may be the primary factor leading to differences in the relaxation parameters among a given set of protein residues. Of course, larger amplitude motion on a time scale slower than overall protein tumbling is also consistent with the present calculations. The effects of motional restriction differ from the variations reflecting differences in diffusion rates and in general a complete set of relaxation parameters should enable at least a partial separation of these effects.

Comparison with a Two-State Model. A variety of models have been proposed recently to describe the relaxation effects produced by internal motion. In general, there are significant qualitative differences which, while not uniquely defining the detailed dynamics of the system, can provide substantial insight into the characteristics of the motion responsible for the observed relaxation parameters. This point may be illustrated by a comparison of the results obtained using the present restricted diffusion model with those obtained from a two-state model in which the relaxation vector is restricted to the orientations $\phi = \pm\theta$. NT_1 values obtained with the parameters $D_0 = 10^7$ s^{-1}, $\beta = 70.53°$, $D_i = 10^{11}$ s^{-1} for the first model and $\tau_A = \tau_B = 1.67 \times 10^{-12}$ s for the second are given in Figure 5. The use of the relation $D_i = 1/(6\tau_A) = 1/(6\tau_B)$ in order to obtain equivalent rates of internal motion is somewhat arbitrary; however, since the condition $D_0 \ll D_i$, $1/\tau_A$, $1/\tau_B$ is satisfied, the calculated relaxation parameters do not depend strongly on the particular choice of internal diffusion rate for either model. The dramatically different dependence of the computed NT_1 values on θ can, in some cases, be used to choose the op-

timal model, thereby providing information on the dynamics of the system under study. For example, we have recently proposed that the internal motion of the proline ring can be described by a two-state model reflecting jumps between the two puckered forms of the molecule.[18] For $\theta = 30°$, a typical displacement for the proline C_γ carbon,[18] NT_1 increases from 65 to 136 ms using the two-state model but only to 83 ms using the restricted diffusion model. An equivalent increase in NT_1 would require $\theta = 55°$ (range = 110°), a physically unacceptable result. These results are consistent with the proposed ring-puckering model and rule out a square-well potential model as being a reasonable representation for the proline molecule.

Conclusions

The effect of restricted internal motion on ^{13}C NMR relaxation parameters is an important practical problem, particularly in studies of large biomolecules. In the present study we have developed a model assuming diffusional motion about an intramolecular bond restricted by the application of infinite boundary conditions. In general the results are physically intuitive; NT_1, NT_2, and NOE values change from the results expected in the absence of internal motion to results close to those expected for free internal motion as the allowed range of motion is increased from 0 to 180°. In a majority of cases corresponding to parameters of practical interest, these changes are monotonic or nearly monotonic. However, for overall motion such that $D_0 \lesssim 10^6$ s^{-1}, nonmonotonic changes of NT_1 and NOE were derived. A useful criterion for application of the present model is the agreement of the relaxation parameters corresponding to a full range of motion, $2\theta = 360°$, with parameters derived using the free internal rotation model. For cases in which this agreement is poor, the detailed results of the calculation appear to be strongly dependent on the boundary conditions applied and the general applicability is suspect. Fortunately, the results obtained for diffusion coefficients down to 10^7 s^{-1} which is a rate expected for small (mol wt 20 000) proteins appear to be well behaved and so should be useful in a number of practical calculations. Application to low molecular weight molecules, e.g., peptides in which motional restriction may be significant, appears to be straightforward. Results applied to the internal motion of methionine residues of dihydrofolate reductase indicate that the restricted motion model can lead to significantly better agreement with experimental data than a model assuming free internal rotations. It should be emphasized, however, that the

present results are not necessarily applicable to relaxation rates obtained for other nuclei. For example, ^1H relaxation rates in proteins appear to be dominated by spin diffusion.[36] This mechanism is inoperative for ^{13}C relaxation under conditions of proton decoupling and assuming poor $^{13}C-^{13}C$ coupling due to dilute spins and the low ^{13}C magnetogyric ratio.

Note Added in Proof. Subsequent to the submission of this manuscript we became aware of an equivalent result obtained by R. J. Wittebort and A. Szabo (*J. Chem. Phys.*, in press). The results obtained are in complete agreement with those presented here. We note further that in the case of successive restricted rotations, it is necessary to specify both the angles between successive rotation axes as well as the direction about which restricted diffusion occurs. For certain cases as discussed here (eq 27–31), this can be accomplished by an appropriate choice of β. More generally, Wittebort and Szabo point out that the inclusion of the Euler angle α provides a convenient means of specifying this parameter.

Appendix A

Using eq 9 and 11 in eq 3 gives a series of terms as a function of the summation index n. Each of these terms can be written as the product of a function of m and the complex conjugate function of m'. The term for $n = 0$ thus has the form $F(m,n = 0)F^*(m', n = 0)$:

$$F(m,n = 0)F^*(m',n = 0)$$
$$= \left[\frac{1}{2\theta} \int_{-\theta}^{\theta} \exp(im\phi_0)d\phi_0 \right]\left[\frac{1}{2\theta} \int_{-\theta}^{\theta} \exp(-im'\phi_t)d\phi_t \right]$$
$$= \frac{\sin m\theta}{m\theta} \frac{\sin m'\theta}{m'\theta} \quad (A1)$$

since the functions are real, $E(m,0) = F(m,0)$.

The remaining terms have the form $F(m,n)F^*(m',n)$ where

$$F(m,n) = \frac{1}{\sqrt{2\theta}} \int_{-\theta}^{\theta} \cos m\phi \cos \left[\frac{n\pi(\phi + \theta)}{2\theta} \right]$$
$$+ i \sin m\phi \cos \frac{n\pi(\phi + \theta)}{2\theta} d\phi \quad (A2)$$

For n odd this becomes

$$F(m,n \text{ odd}) = \frac{(-1)^{(n+1)/2}}{\sqrt{2\theta}} \int_{-\theta}^{\theta} \sin m\phi \sin \left(\frac{n\pi\phi}{2\theta} \right) d\phi$$

$$(A3)$$

For n even this becomes

$$F(m,n \text{ even}) = \frac{(-1)^{n/2}}{\sqrt{2\theta}} \int_{-\theta}^{\theta} \cos m\phi \cos \frac{n\pi\phi}{2\theta} d\phi \quad (A4)$$

It is apparent that the factors $(-1)^{(n+1)/2}$ in eq A3 and $(-1)^{n/2}$ in eq A4 will give 1 in the product $F(m,n)F^*(m,n)$. These factors can thus be dropped in defining $E(m,n)$. Integration

then gives

$$E(m,n \text{ odd}) = \frac{1}{\sqrt{2\theta}} \left[\frac{\sin \left(m\theta - \frac{n\pi}{2} \right)}{m\theta - \frac{n\pi}{2}} - \frac{\sin \left(m\theta + \frac{n\pi}{2} \right)}{m\theta + \frac{n\pi}{2}} \right]$$

$$(A5)$$

$$E(m,n \text{ even}) = \frac{1}{\sqrt{2}} \left[\frac{\sin \left(m\theta - \frac{n\pi}{2} \right)}{m\theta - \frac{n\pi}{2}} + \frac{\sin \left(m + \frac{n\pi}{2} \right)}{m\theta + \frac{n\pi}{2}} \right]$$

$$(A6)$$

These results can be combined to give the results in eq 12 and 14.

References and Notes

(1) D. E. Woessner, *J. Chem. Phys.*, **36**, 1 (1962).
(2) D. E. Woessner, *J. Chem. Phys.*, **37**, 647 (1962).
(3) W. T. Huntress, Jr., *J. Chem. Phys.*, **48**, 3524 (1968).
(4) W. T. Huntress, Jr., *Adv. Magn. Reson.*, **4**, 1 (1970).
(5) Y. Margalit, *J. Chem. Phys.*, **55**, 3072 (1971).
(6) A. Allerhand, D. Doddrell, and R. Komoroski, *J. Chem. Phys.*, **55**, 189 (1971).
(7) D. Doddrell, V. Glushko, and A. Allerhand, *J. Chem. Phys.*, **56**, 3683 (1972).
(8) S. Berger, F. R. Kreissl, D. M. Grant, and J. D. Roberts, *J. Am. Chem. Soc.*, **97**, 1805 (1975).
(9) H. Shimizu, *J. Chem. Phys.*, **37**, 765 (1962).
(10) P. S. Hubbard, *Phys. Rev. A*, **6**, 2421 (1972); 481 (1974); D. E. O'Reilly, *J. Chem. Phys.*, **56**, 2924 (1972).
(11) U. Haeberlen and G. Maier, *Z. Naturforsch., A*, **22**, 1236 (1967); D. C. Look and I. J. Lowe, *J. Chem. Phys.*, **44**, 3437 (1966); B. Ban and C. Chachaty, *Can. J. Chem.*, **51**, 3889 (1973); B. A. Dunell and S. E. Ulrich, *J. Chem. Soc., Faraday Trans 2*, **69**, 377 (1973).
(12) P. Rigny, *Physica (Utrecht)*, **59**, 707 (1972); B. Boddenberg and J. A. Moreno, *Z. Naturforsch., A*, **31**, 854 (1976); B. Boddenberg and J. A. Moreno, *J. Magn. Reson.*, **29**, 91 (1978).
(13) D. E. Woessner, *J. Chem. Phys.*, **42**, 1855 (1965).
(14) D. Wallach, *J. Chem. Phys.*, **47**, 5258 (1967).
(15) (a) D. Ghesquiere, B. Ban, and C. Chachaty, *Macromolecules*, **10**, 743 (1977); (b) T. Yasukawa and C. Chachaty, *Chem. Phys. Lett.*, **43**, 565 (1976); (c) T. Yasukawa, D. Ghesquiere, and C. Chachaty, *ibid.*, **45**, 279 (1977); (d) A. Tsutsumi, *Mol. Phys.*, in press; (e) A. Tsutsumi, B. Perly, A. Forchioni, and C. Chachaty, *Macromolecules*, in press.
(16) W. M. M. J. Bovee and J. Smidt, *Mol. Phys.*, **28**, 1617 (1974).
(17) R. E. London and J. Avitabile, *J. Am. Chem. Soc.*, **99**, 7765 (1977).
(18) R. E. London, *J. Am. Chem. Soc.*, **100**, 2678 (1978).
(19) (a) Y. K. Levine, P. Partington, and G. C. K. Roberts, *Mol. Phys.*, **25**, 497 (1973); (b) Y. K. Levine, N. J. M. Birdsall, A. G. Lee, J. C. Metcalfe, P. Partington, and G. C. K. Roberts, *J. Chem. Phys.*, **60**, 2890 (1974); (c) Y. K. Levine, P. Partington, G. C. K. Roberts, N. J. M. Birdsall, A. G. Lee, and J. C. Metcalfe, *FEBS Lett.*, **23**, 203 (1972); (d) A. G. Lee, N. J. M. Birdsall, J. C. Metcalfe, G. B. Warren, and G. C. K. Roberts, *Proc. R. Soc. London, Ser. B*, **193**, 253 (1976).
(20) Y. K. Levine, *J. Magn. Reson.*, **11**, 421 (1973).
(21) C. H. A. Seiter and S. I. Chan, *J. Am. Chem. Soc.*, **95**, 7541 (1973).
(22) R. L. Blakley, L. D. Cocco, R. E. London, T. E. Walker, and N. A. Matwiyoff, *Biochemistry*, **17**, 2284 (1978).
(23) R. E. London and J. Avitabile, *J. Chem. Phys.*, **65**, 2443 (1976).
(24) K. F. Kuhlman, D. M. Grant, and R. K. Harris, *J. Chem. Phys.*, **52**, 3439 (1970).
(25) R. S. Norton, A. O. Clouse, R. Addleman, and A. Allerhand, *J. Am. Chem. Soc.*, **99**, 79 (1977).
(26) D. J. Wilbur, R. S. Norton, A. O. Clouse, R. Addleman, and A. Allerhand, *J. Am. Chem. Soc.*, **98**, 8250 (1976).
(27) M. E. Rose, "Elementary Theory of Angular Momentum", Wiley, New York, N.Y., 1975.
(28) L. G. Werbelow and D. M. Grant, *J. Chem. Phys.*, **63**, 544 (1975); *ibid.*, **63**, 4742 (1975).
(29) A. Allerhand, D. Doddrell, V. Glushko, D. W. Cochran, E. Wenkert, P. J. Lawson, and F. R. N. Gurd, *J. Am. Chem. Soc.*, **93**, 544 (1971).
(30) E. Oldfield, R. S. Norton, and A. Allerhand, *J. Biol. Chem.*, **250**, 6368 (1975).
(31) R. B. Visscher and F. R. N. Gurd, *J. Biol. Chem.*, **250**, 2238 (1975).
(32) D. Bauer, S. J. Opella, D. J. Nelson, and R. Pecora, *J. Am. Chem. Soc.*, **97**, 2580 (1975).
(33) J. A. McCammon, B. R. Gelin, and M. Karplus, *Nature (London)*, **267**, 585 (1977).
(34) K. Torii and Y. Iitaka, *Acta Crystalogr., Sect. B*, **29**, 2799 (1973).
(35) L. D. Cocco, R. L. Blakley, T. E. Walker, R. E. London, and N. A. Matwiyoff, *Biochemistry*, in press.
(36) A. Kalk and H. J. C. Berendsen, *J. Magn. Reson.*, **24**, 343 (1976).